Magnetic Resonance Imaging 56 (2019) 52–56

Contents lists available at ScienceDirect

Magnetic Resonance Imaging

journal homepage: www.elsevier.com/locate/mri

Original contribution

Restricted self-diffusion of adsorbed water in MIL-100(Al)

Tobias Splith*, Frank Stallmach

University of Leipzig, Faculty of Physics and Earth Science, Linnéstr. 5, 04103 Leipzig, Germany

ARTICLE INFO

Keywords:
PFG NMR
MIL-100(Al)
Restricted diffusion
Two-site exchange
Heat of adsorption

ABSTRACT

An extended two-site exchange model is presented, which is used to evaluate pulsed field gradient (PFG) nuclear magnetic resonance (NMR) measurements of water in the nanoporous metal-organic framework MIL-100(Al). Here the water molecules exchange between the inter- and the intracrystalline space during the observation time, but are also restricted in their movement by the crystal surface. The evaluation of temperature and loading dependent PFG NMR data yields information about the intracrystalline diffusion process, the radius of the restricting geometry and the time constants of the exchange process. The intracrystalline mean residence time is found to decrease with increasing temperature, which allows an estimate of the heat of adsorption under the equilibrium conditions of the NMR measurements.

1. Introduction

The self-diffusion of adsorbed molecules in a porous material can be used to characterize the interactions between the molecules and the host system. An important nondestructive method to study self-diffusion is pulsed field gradient nuclear magnetic resonance (PFG NMR) [1,2]. It probes the diffusion over a time interval starting at some milliseconds up to times limited only by nuclear relaxation. The resulting PFG NMR signal is the Fourier transform of the mean propagator describing the diffusion of the adsorbed molecules through the heterogeneous system. It, therefore, carries information about the diffusion process and especially about the different obstacles the molecules encounter on their diffusion path during the observation time, e.g. a restricting geometry [3,4]. The influence of such restricting geometries on the mean diffusion coefficient strongly depends on the number of molecules encountering them and, therefore, on the observation time itself.

In a heterogeneous sample the diffusion of the molecules is influenced by an exchange between different regions (sites) consisting, e.g., of the pore space in porous particles and the void space surrounding the particle. In order to describe such a two-site exchange, Kärger developed a model [5,6], which accounts for two different sites with respective mean residence times, diffusion coefficients and relaxation times. In [7] we recently extended this model to the case of anisotropic diffusion in the intracrystalline pore space. A comparable approach will be used in this work in order to describe the diffusion of water in the nanoporous metal-organic framework (MOF) MIL-100(Al).

MIL-100 was first characterized in its chromium form by Férey et al. [8]. It consist of supertetrahedra formed by trimers of metallic cations and the organic linker benzene-1,3,5-tricarboxylate. The resulting pore space contains two kinds of pores: small pores of approximately 2.5 nm diameter and larger pores of 2.9 nm diameter. The aluminum form of MIL-100 was described by Volkringer et al. [9], where the interested reader may also find a graphical representation of the pore structure. Many studies of other forms of MIL-100 with different metallic cations can be found in literature, see e.g. references [10-13].

Due to its high stability and adsorption enthalpy, MIL-100(Al) is a promising material for adsorptive heat transformation applications, where the heat of adsorption of a working fluid (water) is utilized in a thermodynamic cycle. In [14] studies of the diffusion of water MIL-100(Al) by PFG NMR and molecular dynamic simulations (MD simulations) are presented. The PFG NMR data show evidence of both, a restriction effect at the crystal boundaries and an exchange between the porous crystals and the gas phase surrounding the crystals. The intracrystalline diffusion coefficient was extracted by fitting the PFG NMR data with a monoexponential function at high attenuations, where the signal can be attributed to the molecules remaining in one crystal over the whole observation time.

In this paper we evaluate the PFG NMR data of water in MIL-100(Al) by using an extended two-site exchange model. We will show that this alternative approach allows us to describe the complete set of spin echo attenuations measured at different observation times with one equation, resulting in a reduced number of total fit parameters and additional information on the system under study. For experimental details about the synthesis of the MIL-100(Al) crystals, the loading procedure and the PFG NMR measurements the reader is referred to [14].

* Corresponding author.
E-mail address: Tobias.Splith@physik.uni-leipzig.de (T. Splith).

https://doi.org/10.1016/j.mri.2018.09.001
Received 12 June 2018; Received in revised form 2 September 2018; Accepted 2 September 2018

2. Materials and methods

2.1. Restricted diffusion

For self-diffusion restricted inside spheres of a radius R, the propagator can be found in a publication of Neuman [15]. Balinov et al. [3] use this propagator to describe the spin echo attenuation curve of respective molecules with

$$\Psi_R(q,\Delta) = \frac{9(qR\cos qR - \sin qR)^2}{(qR)^6} + 6q^2R^2\sum_{n=0}^{\infty}\left(n\frac{j_n(qR)}{qR} - j_{n+1}(qR)\right)^2 \sum_{m=1}^{\infty}\frac{(2n+1)\alpha_{nm}^2}{\alpha_{nm}^2 - n^2 - n}\exp\left\{-\frac{\alpha_{nm}^2 D_0\Delta}{R^2}\right\}\frac{1}{(\alpha_{nm}^2 - q^2R^2)^2} \quad , \tag{1}$$

where q is the absolute value of the **q**-vector related to the gradient intensity and duration applied during the PFG NMR experiment, $j_n(x)$ is the spherical Bessel function of the first kind and of n-th order and α_{nm} is the m-th root of the equation

$$f(\alpha) = n\frac{j_n(\alpha)}{\alpha} - j_{n+1}(\alpha) \quad . \tag{2}$$

D_0 is the purely intracrystalline diffusion coefficient, i.e. the diffusion coefficient of the molecules that did not encounter the surface barrier during the observation time Δ.

For small values of q Eq. (1) can be approximated with

$$\Psi(q,\Delta) \approx \exp\{-q^2\Delta D_{\text{eff}}\} \quad , \tag{3}$$

where D_{eff} represents the effective or mean diffusion coefficient [16]

$$D_{\text{eff}}(\Delta) = -\frac{1}{\Delta}\lim_{q\to 0}\frac{\partial \ln\Psi(q,\Delta)}{\partial(q^2)} \quad . \tag{4}$$

There are two limits in which this effective diffusion coefficient can be described by rather simple equations: For large values of the observation time Δ, where the diffusion process is no longer influenced by the intracrystalline diffusion coefficient D_0 but purely by the dimensions of the restricting geometry, the effective diffusion coefficient will be asymptotic to the equation

$$D_{\text{eff}}(\Delta) = \frac{R^2}{5\Delta} \quad . \tag{5}$$

In the limit of short observation times the influence on the effective diffusion coefficient was studied by Mitra et al. [4]. For a spherical surface the second order approximation of the effective diffusion coefficient is given by

$$D_{\text{eff}}(\Delta) = D_0\left(1 - \frac{4}{3}\frac{1}{\sqrt{\pi}}\sqrt{\frac{D_0\Delta}{R^2}} - \frac{1}{2}\frac{D_0\Delta}{R^2}\right) \quad . \tag{6}$$

Fig. 1 shows the relative effective diffusion coefficient as a function of the effective observation time $\frac{D_0\Delta}{R^2}$ for the exact representation of the spin echo attenuation (Eq. (1)) and for both approximations (Eqs. (5) and (6)). Only for values of $0.1 < \frac{D_0\Delta}{R^2} < 1.0$ the effective diffusion coefficient can not be described by either of the two approximations.

For data analysis we will approximate the MIL-100(Al) crystals under study to be spherical and use Eq. (1) to describe the spin echo attenuation of adsorbed water restricted in its diffusion by the external crystal surface. The radii of the spheres should be related to the size of the MIL-100(Al) crystals, which was found to be between 4 and 10 µm (see SEM micrograph in Fig. S7 in the supporting information of [14]).

2.2. The two-site exchange model with restricted intracrystalline diffusion

The exchange model of Kärger [5,6] considers two sites with

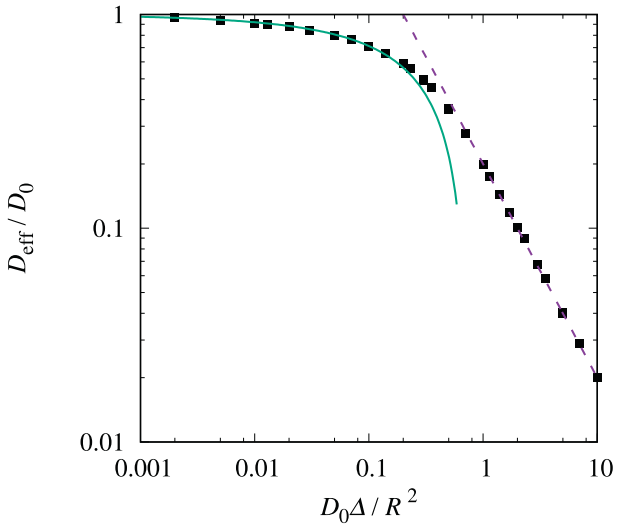

Fig. 1. The relative effective diffusion coefficient for diffusion inside a sphere of the radius R plotted as a function of the effective observation time. The black squares are calculated with the approximation of low q-values (Eq. (4)) from the exact representation of the spin echo attenuation given in Eq. (1). The dashed line represents the approximation for high observation times (Eq. (5)), while the continuous green line refers to the second order approximation at low observation times (Eq. (6)). (For interpretation of the references to color in this figure legend, the reader is referred to the web version of this article.)

isotropic and unrestricted diffusion, respectively. In [7] this model was extended to the case of anisotropic diffusion in the intracrystalline space by inserting the mean propagator of the anisotropic diffusion into the respective equations. For the PFG NMR data analysis of water in MIL-100(Al) we apply exactly the same procedure using however the Fourier transform of the propagator of diffusion inside a sphere (Eq. (1)). In this way the contribution of the diffusion to the spin echo attenuation is continuously described for all values of the effective observation time $\frac{D_0\Delta}{R^2}$, capturing the whole range from free to completely restricted intracrystalline diffusion (see Fig. 1).

The extended model calculates the contribution to the spin echo attenuation of a group of molecules that is defined by the exchange times (t_1,t_2,t_3,…,t_n) during the experiment and by the site in which the molecules were at the beginning of the experiment. Consider for example molecules that are in the intracrystalline space at the beginning of the experiment t_0, exchange at a fixed time t_1 into the intercrystalline space, exchange back into the intracrystalline space at a fixed time t_2 and remain there until the experiment ends ($t = \Delta$). Until $t = t_1$ the diffusion of these molecules can be described by the propagator of restricted diffusion inside a sphere with reflecting boundaries. From $t = t_1$ to $t = t_2$ the molecules can diffuse freely in the intracrystalline space. At $t = t_2$ they will enter the intracrystalline space, where their diffusion can again be described by the propagator of restricted diffusion until $t = \Delta$. The relative amount of molecules with these respective exchange times is calculated as a function of the mean residence times τ_a and τ_b. By integrating over all possible exchange times, the model yields the spin echo attenuation curves of all the molecules in the system. This integration is done numerically. For further detail the reader is referred to the supporting information of [7].

In this rather simplistic model, the molecular exchange between the intracrystalline phase (a) and the surrounding gas phase (b) is represented by the mean residence times τ_b and τ_a, respectively, and not by the history of the individual diffusing molecules. This might cause a discrepancy to the real system, where there might be a correlation of the mean residence times, i.e. molecules that have exchanged recently might be more probable to exchange again a short time later than other molecules since they are near a crystal surface. Nonetheless, we will

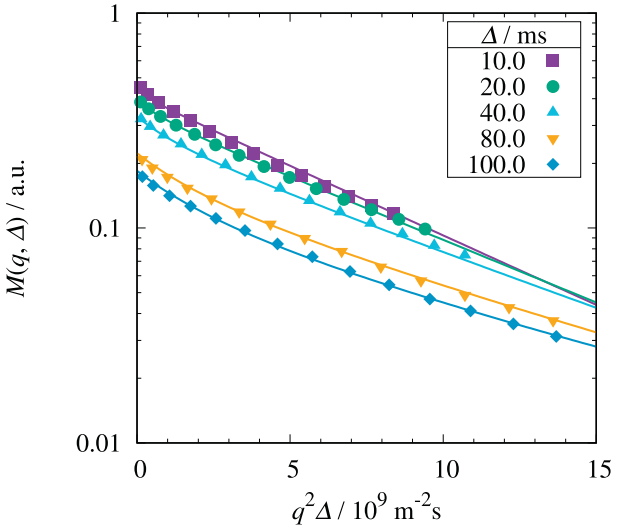

Fig. 2. Spin echo-attenuation of water in MIL-100(Al) measured at multiple observation times Δ as indicated in the figure. The lines represent a fit of the whole dataset with the extended two-site exchange model.

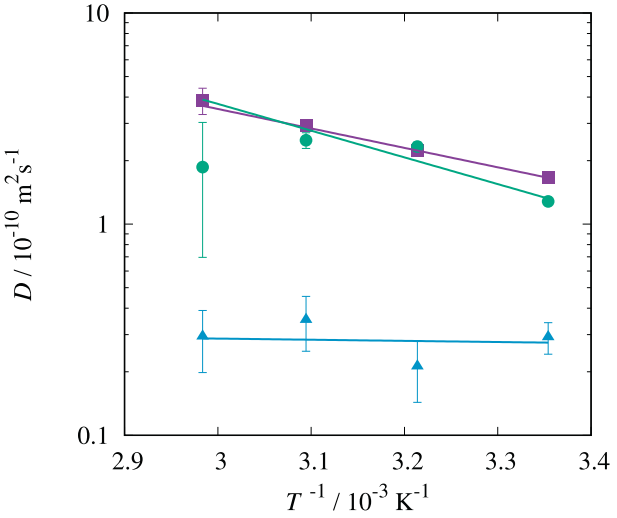

Fig. 3. Diffusion coefficient of water in MIL-100(Al) measured at multiple loadings (0.60 g/g: purple, 0.32 g/g: green, 0.17 g/g: blue) plotted as a function of the inverse temperature. The lines represent fits with the Arrhenius equation (Eq. (7)). (For interpretation of the references to color in this figure legend, the reader is referred to the web version of this article.)

apply this extended model to evaluate the experimental PFG NMR data.

2.3. Experimental details

The PFG NMR studies were performed at the FEGRIS NT spectrometer operating at a ^{1}H-resonance frequency of 125 MHz [1] which is equipped with a house build gradient coil [17]. Diffusion measurements were performed for loadings of 0.6 g/g, 0.32 g/g and 0.17 g/g at four different temperatures between 298 K and 335 K. The observation time of the PFG NMR experiments Δ was varied from 10 ms to 100 ms. Further information about loading of the samples and the experimental procedure can be found in [14].

3. Results and discussion

Fig. 2 shows the spin echo attenuation curves measured at $T = 298$ K and a loading of $a = 0.60$ g/g from [14] evaluated with the extended exchange model, which considers restricted diffusion in the intracrystalline phase and isotropic diffusion in the vapor phase. The whole set of data is evaluated with a single fit. Variable parameters are the intracrystalline diffusion coefficient D_0, the mean residence times τ_a and τ_b, the mean radius of the restricting geometry R, the signal intensity M_0 and an offset o, which considers the noise level of the PFG NMR experiment. Fixed parameters of the evaluation are, similar to the evaluation shown in [7], the isotropic diffusion coefficient in the

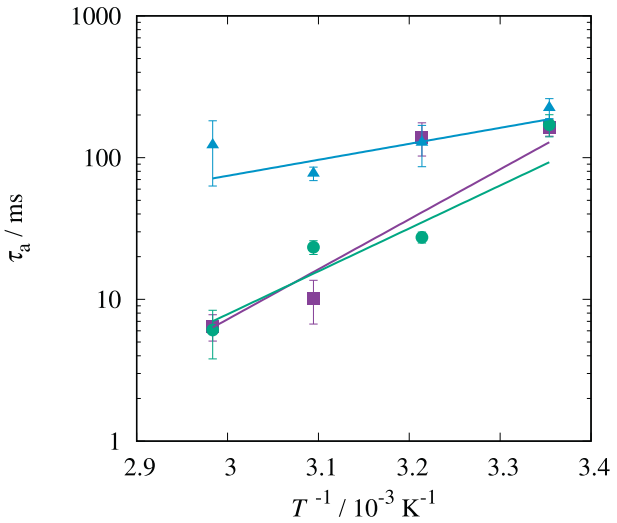

Fig. 4. Mean intracrystalline residence times of water in MIL-100(Al) at multiple loadings (0.60 g/g: purple, 0.32 g/g: green, 0.17 g/g: blue) plotted as a function of the inverse temperature. The lines represent fits with the Arrhenius equation (Eq. (8)). (For interpretation of the references to color in this figure legend, the reader is referred to the web version of this article.)

Table 1
Evaluation parameters obtained with the extended exchange model from PFG NMR data measured for water in MIL-100(Al) at multiple temperatures and loadings. The uncertainties shown are the standard deviation of the fit parameters obtained by the nonlinear least-squares Marquardt-Levenberg algorithm.

a/g/g	T/K	$D_a/10^{-10}$ m^2 s^{-1}	τ_a/ms	τ_b/μs	R/μm	M_0	$o/10^{-3}$
0.60	298	1.66 ± 0.03	163 ± 22	1.1 ± 0.3	8.3 ± 0.4	0.59 ± 0.01	12 ± 4
0.60	311	2.23 ± 0.01	139 ± 37	1.2 ± 0.5	15 ± 5	0.56 ± 0.01	7 ± 2
0.60	323	2.9 ± 0.2	10 ± 4	0.01 ± 0.03	6 ± 3	0.55 ± 0.01	14 ± 1
0.60	335	3.9 ± 0.5	6.4 ± 1.4	0.01 ± 0.03	4.3 ± 0.2	0.49 ± 0.02	12 ± 1
0.32	298	1.28 ± 0.05	170 ± 30	0.48 ± 0.14	7.1 ± 0.1	0.34 ± 0.01	4 ± 1
0.32	311	2.33 ± 0.11	27 ± 3	0.18 ± 0.02	3.3 ± 0.2	0.32 ± 0.01	2.4 ± 0.3
0.32	323	2.5 ± 0.2	23 ± 3	0.34 ± 0.05	3.5 ± 0.4	0.26 ± 0.01	2.0 ± 0.3
0.32	335	1.9 ± 1.2	6 ± 3	0.11 ± 0.04	3 ± 2	0.28 ± 0.01	9.1 ± 0.5
0.17	298	0.39 ± 0.05	220 ± 40	8.0 ± 5	–	0.20 ± 0.01	3 ± 1
0.17	311	0.21 ± 0.07	130 ± 40	0.7 ± 0.4	–	0.16 ± 0.01	8 ± 1
0.17	323	0.35 ± 0.10	77 ± 8	300 ± 70	–	0.27 ± 0.01	6.0 ± 0.6
0.17	335	0.29 ± 0.10	120 ± 60	0.6 ± 0.5	–	0.15 ± 0.01	4 ± 2

intercrystalline gas phase, which can be estimated with the Chapman-Enskog theory [18] ($D_b = 2.86 \times 10^{-5}\,m^2\,s^{-1}$ at $T = 298\,K$), and the relaxation times, which were measured independently with the CPMG and the inversion recovery pulse sequence ($T_{1,a} = 100.4\,ms$ and $T_{2,a} = 2.4\,ms$ at $T = 298\,K$ and $a = 0.60\,g/g$, for relaxation times at other conditions see Table S3 in the supporting information of [14]).

The data analysis with the extended two-site exchange model describes the whole set of PFG NMR data very well (see Fig. 2). It represents a significant improvement compared to the evaluation in [14], where only the effective intracrystalline diffusion coefficient was extracted with a fit at high $q^2\Delta$-values.

The same evaluation procedure was applied to PFG NMR data measured at different loadings and temperatures. In Table 1 the experimental conditions and the resulting fit parameters are shown.

Fig. 3 shows the diffusion coefficient obtained for multiple loadings as a function of the inverse temperature. The data is evaluated with the Arrhenius equation

$$D(T) = D_\infty \exp\left\{-\frac{E_D}{RT}\right\} \quad . \tag{7}$$

Under the assumption that the diffusion is an activated process, this evaluation yields the activation energy E_D of the diffusion process, which represents the energetic barrier between the adsorption sites inside the nanopores. At loadings of 0.60 g/g and 0.32 g/g the resulting activation energies are $E_D = (18 \pm 1)\,kJ/mol$ and $E_D = (24 \pm 7)\,kJ/mol$, respectively. At a loading of 0.18 g/g, due to the higher experimental uncertainty of the diffusion coefficients, no reliable value for E_D could be obtained, but one can clearly see that the activation energy is smaller than at high loadings. A similar behavior was already reported in [14] and analyzed by MD simulations. It is the result of water molecules being primary adsorbed in the small pores of MIL-100(Al). Only at high loadings the water molecules can access the center of the large pores. This leads to an increase of both, the diffusion coefficient and the activation energy of the diffusion process with increasing loading.

Fig. 4 shows the mean intracrystalline residence time τ_a of water in the MIL-100(Al) crystals as a function of the inverse temperature. With the assumptions that the exchange between the intracrystalline adsorbed phase and the surrounding gas phase is an activated process and that the exchange is not limited by the intracrystalline diffusion, this data can be evaluated with an Arrhenius equation

$$\tau(T) = \tau_0 \exp\left\{\frac{E_{ex}}{RT}\right\} \tag{8}$$

as well. The activation energy of the exchange process E_{ex} is related to the heat of adsorption. Within the uncertainties of the measurements and the data analysis the resulting energies of $E_{ex} = (68 \pm 18)\,kJ/mol$, $E_{ex} = (58 \pm 17)\,kJ/mol$ measured at loadings of 0.60 g/g and 0.32 g/g, respectively, are in agreement with the heats of adsorption of 46 kJ/mol measured with adsorption experiments [19] and of 54 kJ/mol estimated with Monte Carlo simulation [14]. At a loading of $a = 0.18\,g/g$ evaluation of the observation times yields an activation energy of $E_{ex} = (22 \pm 13)\,kJ/mol$. This lower activation energy may be attributed to the lower diffusion coefficient at this loading and, therefore, to a diffusive limitation of the exchange process.

At loadings of $a = 0.60\,g/g$ and 0.32 g/g the extended two-site exchange model yields values for the average radius of the restricting geometry, while at lower loadings no reliable value for this parameter could be found. This is caused by the decreased diffusivity D_0 at these loadings, which result in a lower effective observation time $\frac{D_0\Delta}{R^2}$ and, therefore in a significantly smaller influence of the restriction (see Fig. 3). The values obtained for R are in the same order of magnitude as the crystal sizes estimated from SEM micrographs shown in the supporting information of [14].

4. Conclusion

We applied an extended two-site exchange model to the PFG NMR data measured with water in the nanoporous MIL-100(Al). The model accounts for an exchange between molecules adsorbed in nanoporous crystals and the surrounding gas phase and considers the restricting effect on the outer surface of the crystals. The spin echo attenuation curves are well represented by the extended model and only one joint fit is needed to evaluate a whole set of PFG NMR data measured at multiple observation times. In addition to the intracrystalline diffusion coefficient, the evaluation with the extended two-site model yields values for the mean residence times on both sites and for the radius of the restricting geometry.

From the temperature dependency of the diffusion coefficients the activation energy of the diffusion process can be estimated. A significant increase of this energy and of the diffusion coefficient is seen with increasing loadings. These observations are consistent with the results of molecular dynamics simulations of water in MIL-100(Al) [14] and can be attributed to the larger pores of MIL-100(Al) being only accessible at high loadings.

The temperature dependency of the intracrystalline mean residence time obtained with the extended two-site exchange model was used for an estimation of the activation energy of the exchange. If the exchange is not limited by the intracrystalline diffusion the activation energy of the exchange corresponds to the heat of adsorption of water in MIL-100(Al) under equilibrium conditions.

Acknowledgments

We thank our cooperation partners of Fraunhofer ISE Freiburg (Germany) and NTU Athens (Greece) for sharing MIL-100(Al) data within the Greek-German collaborative research Project WasserMod. The authors acknowledge the financial support by the Federal Ministry of Education and Research of Germany in the framework of WasserMod (project number 03SF0469A).

References

[1] Stallmach F, Galvosas P. Spin echo NMR diffusion studies. Annu Rep NMR Spectrosc 2007;61:51–131.
[2] Kärger J, Ruthven D, Theodorou D. Diffusion in nanoporous materials. Wiley; 2012. URL https://books.google.de/books?id=g0sxMMliOYQC.
[3] Balinov B, Jonsson B, Linse P, Soderman O. The NMR self-diffusion method applied to restricted diffusion. Simulation of echo attenuation from molecules in spheres and between planes. J Magn Reson Ser A 1993;104(1):17–25. https://doi.org/10.1006/jmra.1993.1184. URL http://www.sciencedirect.com/science/article/pii/S1064185883711848.
[4] Mitra P P, Sen P N, Schwartz L M. Short-time behavior of the diffusion coefficient as a geometrical probe of porous media. Phys Rev B 1993;47:8565–74. https://doi.org/10.1103/PhysRevB.47.8565. URL https://link.aps.org/doi/10.1103/PhysRevB.47.8565.
[5] Kärger J. Determination of diffusion in a 2 phase system by pulsed field gradients. Ann Phys 1969;24(1–2):1.
[6] Kärger J. Influence of 2-phase diffusion on spin-echo attenuation regarding relaxation in measurements using pulsed field gradients. Ann Phys 1971;27(1):107.
[7] Splith T, Fröhlich D, Henninger S K, Stallmach F. Development and application of an exchange model for anisotropic water diffusion in the microporous MOF aluminum fumarate. J Magn Reson 2018;291:40–6. https://doi.org/10.1016/j.jmr.2018.04.009. URL http://www.sciencedirect.com/science/article/pii/S1090780718301137.
[8] Férey G, Christian S, Caroline M, Franck M, Suzy S, Julien D. A hybrid solid with giant pores prepared by a combination of targeted chemistry, simulation, and powder diffraction. Angew Chem Int Ed 2004;43(46):6296–301. https://doi.org/10.1002/anie.200460592. URL https://onlinelibrary.wiley.com/doi/abs/10.1002/anie.200460592.
[9] Volkringer C, Popov D, Loiseau T, Férey G, Burghammer M, Riekel C. Synthesis, single-crystal X-ray microdiffraction, and NMR characterizations of the giant pore metal-organic framework aluminum trimesate MIL-100. Chem Mater 2009;21(24):5695–7. https://doi.org/10.1021/cm901983a. URL https://doi.org/10.1021/cm901983a.
[10] Horcajada P, Surble S, Serre C, Hong D-Y, Seo Y-K, Chang J-S. Synthesis and catalytic properties of MIL-100(Fe), an iron(III) carboxylate with large pores. Chem Commun 2007:2820–2. https://doi.org/10.1039/B704325B. URL http://dx.doi.org/10.1039/B704325B.

[11] Mowat J P, Miller S R, Slawin A M, Seymour V R, Ashbrook S E, Wright P A. Synthesis, characterisation and adsorption properties of microporous scandium carboxylates with rigid and flexible frameworks. Microporous Mesoporous Mater 2011;142(1):322–33. https://doi.org/10.1016/j.micromeso.2010.12.016. URL http://www.sciencedirect.com/science/article/pii/S138718111000449X.

[12] Lieb A, Leclerc H, Devic T, Serre C, Margiolaki I, Mahjoubi F. MIL-100(V) - a mesoporous vanadium metal organic framework with accessible metal sites. Metal Organic Frameworks Microporous Mesoporous Mater 2012;157:18–23. https://doi.org/10.1016/j.micromeso.2011.12.001. URL http://www.sciencedirect.com/science/article/pii/S1387181111005841.

[13] Reinsch H, Stock N. Formation and characterisation of Mn-MIL-100. CrystEngComm 2013;15:544–50. https://doi.org/10.1039/C2CE26436F. URL http://dx.doi.org/10.1039/C2CE26436F.

[14] Splith T, Pantatosaki E, Kolokathis P D, Fröhlich D, Zhang K, Füldner G. Molecular dynamics phenomena of water in the metalorganic framework MIL-100(Al), as revealed by pulsed field gradient NMR and atomistic simulation. J Phys Chem C 2017;121(33):18065–74. https://doi.org/10.1021/acs.jpcc.7b06240. URL http://dx.doi.org/10.1021/acs.jpcc.7b06240.

[15] Neuman C H. Spin echo of spins diffusing in a bounded medium. J Chem Phys 1974;60(11):4508–11. https://doi.org/10.1063/1.1680931. URL arXiv:https://doi.org/10.1063/1.1680931.

[16] Price W S, Barzykin A V, Hayamizu K, Tachiya M. A model for diffusive transport through a spherical interface probed by pulsed-field gradient NMR. Biophys J 1998;74(5):2259–71. https://doi.org/10.1016/S0006-3495(98)77935-4.

[17] Schlayer S, Stallmach F, Horch C, Splith T, Pusch A, und M Peksa F P. Konstruktion und test eines gradientensystems für NMR-diffusionsuntersuchungen in grenzflächensystemen. Chem Ing Tech 2013;85:1–7. (In German).

[18] Hirschfelder J, Curtiss C, Bird R. U. of Wisconsin. Theoretical Chemistry Laboratory. Molecular theory of gases and liquids. Structure of matter series. Wiley; 1954. URL https://books.google.de/books?id=HQtRAAAAMAAJ.

[19] Jeremias F, Khutia A, Henninger S K, Janiak C. Mil-100(Al, Fe) as water adsorbents for heat transformation purposes-a promising application. J Mater Chem 2012;22:10148–51. https://doi.org/10.1039/C2JM15615F. URL http://dx.doi.org/10.1039/C2JM15615F.